

## Integrated PIC-fluid modeling of the melting experiments of the WEST tokamak monoblocks

F. Cichocki<sup>1</sup>, G. Rubino<sup>2</sup>, L. Balbinot<sup>3,5</sup>, F. Taccogna<sup>2</sup>, J. Gerardin<sup>4</sup>, Q. Tichit<sup>4</sup>, J.P. Gunn<sup>4</sup>, Y. Corre<sup>4</sup>, the WEST team<sup>\*</sup>, and the EUROfusion Tokamak Exploitation Team<sup>\*\*</sup>

<sup>1</sup> ENEA C.R. Frascati, "Nuclear" Department, Frascati, Rome, Italy

<sup>2</sup> Istituto per la Scienza e Tecnologia dei Plasmi (ISTP-CNR), Bari, Italy

<sup>3</sup> Università della Tuscia, Viterbo, Italy

<sup>4</sup> CEA, IRFM, F-1308 Saint-Paul-les-Durance Cedex, France

<sup>5</sup> DTT S.c.a.r.l., Frascati, Rome, Italy

<sup>\*</sup> See <https://irfm.cea.fr/en/west/WESTteam/>

<sup>\*\*</sup> See the author list of E.Joffrin et al 2024 Nucl.Fusion 64 112019,

<https://doi.org/10.1088/1741-4326/ad2be4>

During the WEST 2024 C9 experimental campaign, a set of experiments was carried out to characterize the physical damage on divertor monoblocks exposed to a parallel energy flux at the outer strike point, as in [1][2]. As shown in Figure 1, this was achieved by grooving the monoblock #28 of the PFU#6, thus exposing the toroidally adjacent monoblock of the PFU#7 to very high parallel energy fluxes. Two experiments were completed: a preparatory one featuring a parallel heat flux lower than the minimum required for melting ( $<100 \text{ MW/m}^2$ ), and a melting one with parallel heat fluxes higher than  $100 \text{ MW/m}^2$ . The wall temperature of PFU#7 was estimated from IR thermography, while a set of Langmuir probes located in proximity of the strike point was used to evaluate the plasma properties close to the wall.

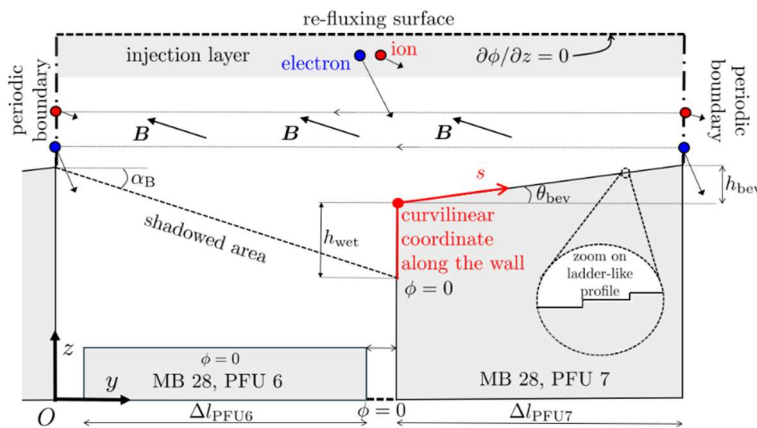


Figure 1: Experimental setup and DESPICCO simulation domain, showing the grooved monoblock (MB #28, PFU #6) and the exposed vertical area on the target monoblock (MB #28, PFU #7), at the outer divertor strike point. The horizontal direction is along the machine toroidal coordinate.

For a better understanding of the experiments, an accurate model of the plasma-material

interaction is needed, accounting for effects such as the local electric currents reaching the monoblock, magnetic and Debye sheaths forming close to the wall, finite ion Larmor radius effects, thermionic and secondary electron emission and plasma particles collisions with recycled neutrals. This has been achieved by combining axisymmetric scrape-off layer (SOL) fluid codes with the kinetic particle-in-cell (PIC) code DESPICCO [3]. While SOL codes identify plasma conditions at the wall close to the strike point, the PIC code simulates the last mms of the plasma-wall interaction consistently at the poloidal peak flux location, including

the above-mentioned effects and assuming the correct toroidal shaping of the monoblocks [4]. These PIC simulations cover the plane containing the toroidal and normal-to-wall directions, thus permitting to evaluate correctly the effects of monoblock shadowing and beveling.

### Inputs from scrape-off-layer codes

The SOL plasma of the preparatory experiment has been simulated with the SOLPS-ITER code suite [5][6]. The power crossing the separatrix has been fixed to 2 MW, as derived from experiments, and the full set of O ionization stages has been modeled as a proxy for the intrinsic impurity. The cross-field transport parameters and the outer midplane separatrix density, equal to  $1.9 \cdot 10^{19} \text{ m}^{-3}$ , have been optimized to match the Langmuir probe data at the outer target and the divertor radiation along bolometry lines of sight. The SOL plasma of the melting experiment has been simulated with the SOLEDGE2D-EIRENE coupled code [7]. Modelling has been carried out in deuterium only (no impurities), scanning over the total particle power crossing the separatrix  $P_{\text{in}}$  and the outer mid-plane separatrix density  $n_{\text{e,sep}}$ . The best matching with experiments has been obtained for  $n_{\text{e,sep}} = 2.7 \cdot 10^{19} \text{ m}^{-3}$  and  $P_{\text{in}} = 1.9 \text{ MW}$ . Figure 2 finally shows the achieved matching between simulations and experiments.

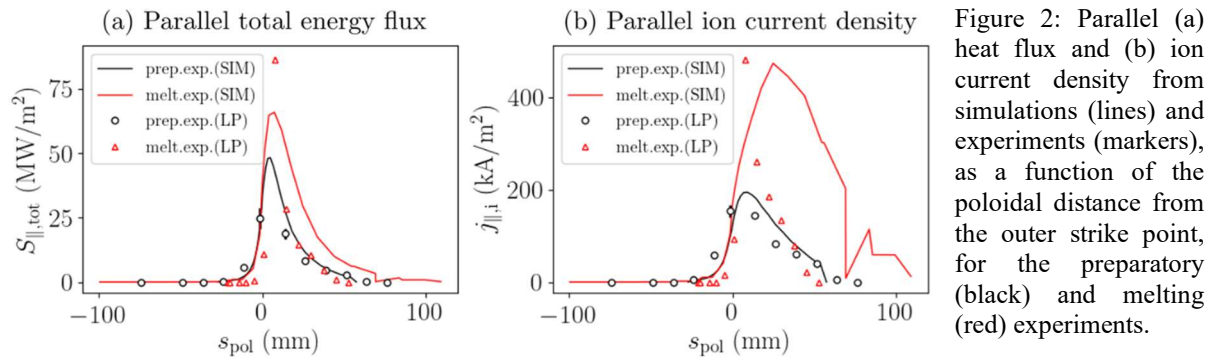


Figure 2: Parallel (a) heat flux and (b) ion current density from simulations (lines) and experiments (markers), as a function of the poloidal distance from the outer strike point, for the preparatory (black) and melting (red) experiments.

### Particle-in-cell model and results

The PIC model considers pure deuterium plasma, with a homogeneous and fixed D neutral background and requires the following inputs (from SOL codes and experiments): electron and ion fluxes from the bulk plasma, electron and ion temperatures, neutral background density, and the wall temperature profile. Referring to Figure 1, the 2D PIC domain is periodic along the toroidal direction  $y$ , and the correct wet surface extension on PFU#7 is achieved by adjusting the length of the previous PFU#6,  $\Delta l_{\text{PFU}6}$ . Due to the periodicity assumption, particles traversing the left and right boundaries are periodically reflected on the other side. Particles are injected from an injection layer next to the upper boundary (grey region in Figure 1): electrons and ions are injected following a Maxwellian flux distribution [3], with the latter featuring a fluid velocity anti-parallel to the magnetic field and equal in magnitude to the ion

sound speed. The upper boundary also acts as a refluxing surface, meaning that any particle traversing it upwards is re-injected with the injection distribution function. A homogeneous Neumann condition is applied to the electric potential there. Inside the plasma volume, particle collisions are simulated following a Monte Carlo Collisions approach [3][4] including (i) elastic and charge transfer collisions between  $D^+$  and  $D$ , and (ii) elastic, excitation, and ionization collisions of electrons with  $D$ . At the monoblocks surface, the electric potential  $\phi$  is set to 0, while the simulated plasma-wall interaction processes are the (i) electron-induced secondary electron emission, and (ii) the thermionic electron emission [3]. For the latter, the Richardson-Dushman formula [3] is considered for a given wall temperature profile, which is shown in Figure 3(a,b) for both experiments. In the plots,  $s < 0$  refers to the vertical exposed surface and  $s > 0$  to the tilted horizontal surface.

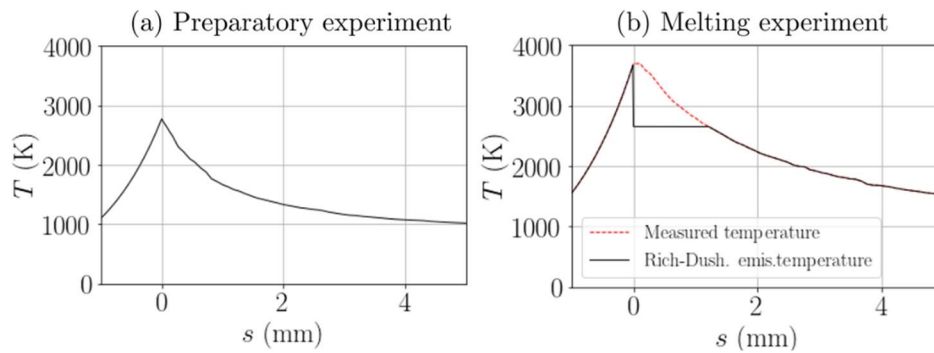


Figure 3: Assumed wall temperature profile for the (a) preparatory and (b) melting experiments.

In the melting experiment, the tungsten melting temperature (3695 K) is reached at  $s = 0$ , and the imposed temperature differs from the measured one whenever thermionic saturation conditions are reached [8]. This approach allows simulating correctly the total emitted current, without further refining the mesh to simulate an inverse sheath formation. Finally, in the melting experiment scenario only, any thermionically emitted electron is not refluxed at the upper boundary, thus yielding a net electric current from the plasma to the wall (as observed experimentally).

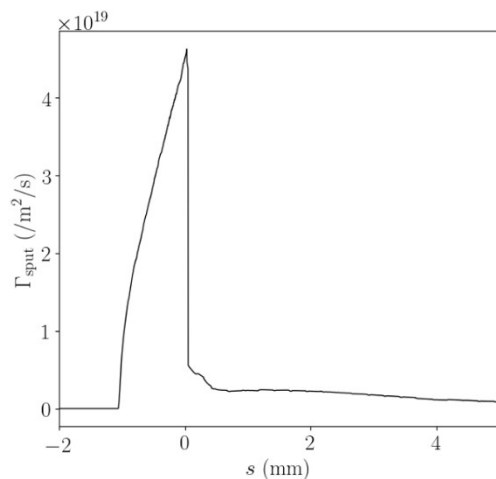


Figure 4: Sputtered tungsten flux along the wall emitted by the exposed monoblock, in the preparatory experiment.

Figure 4 shows the PIC results for the sputtered W flux from the wall, in the preparatory experiment. The sputtering yield dependence on the ion impact angle and energy of Eckstein's model [9][10] ( $D$  on  $W$ ) has been considered. Fluxes are in line with the available integral visible spectroscopy measurements (in the order of  $10^{19}\text{m}^{-2}\text{s}^{-1}$ ).

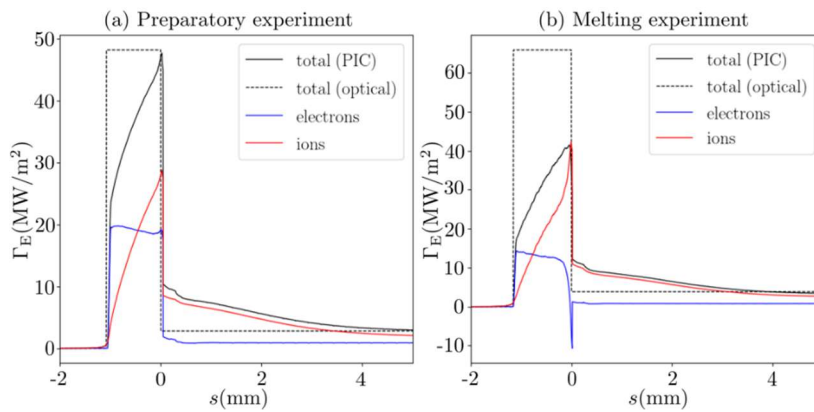


Figure 5: Energy fluxes to wall in (a) preparatory and (b) melting experiments. Shown results in (b) are not fully steady-state.

The total energy fluxes to the wall are finally shown in Figure 5(a,b) for both experiments. The ion energy flux departs considerably from the optical approximation, yielding to a generally lower energy flux on the vertical exposed surface and a higher flux on the beveled horizontal one. The effect of the strong thermionic emission is finally very patent in the melting experiment, where a negative electron energy flux is found very close to the edge ( $s \approx 0$ ).

### Conclusions and future work

An integrated modeling approach, combining fluid codes for the SOL and a 2D-3V PIC code for the plasma-wall interaction at the poloidal heat flux peak, has been presented for the WEST melting experiments. Regarding the SOL modeling, a good preliminary match with experiments has been obtained. Future work will focus on improving such an agreement, especially in the melting scenario, by adding oxygen as a proxy for medium-Z impurities. Regarding the PIC modeling, results show that the optical approximation is affected by large errors in the energy fluxes spatial distributions and that thermionic emission can significantly affect these, when melting occurs. Simulated sputtered fluxes are in line with available sputtering measurements, however, since no spatially-resolved data are available, a new preparatory-like experiment would be needed to validate the PIC code. Furthermore, the PIC spatial distributions of the energy flux will be used in a dedicated monoblock thermal model to obtain its temperature distribution and compare it against available IR experimental data.

### Acknowledgments and references

*This work has been carried out within the framework of the EUROfusion Consortium, funded by the European Union via the Euratom Research and Training Programme (Grant Agreement No 101052200 — EUROfusion). Views and opinions expressed are however those of the author(s) only and do not necessarily reflect those of the European Union or the European Commission. Neither the European Union nor the European Commission can be held responsible for them*

- |   |  |
|---|--|
| [1] S.Ratynskaia et al, Nucl.Mater.Energy <b>33</b> :101303,2022        | [6] D.Reiter et al, Fusion Sci.Technol. <b>47</b> :172–86,2005   |
| [2] Y.Corre et al, Phys. Scr. <b>96</b> (12):124057,2021                | [7] H.Bufferand et al, J.Nucl.Mater. <b>438</b> :S445-S448,2013  |
| [3] F.Cichocki et al, Nucl. Fusion <b>63</b> :086022,2023               | [8] M.Komm et al, Nucl. Fusion <b>60</b> :054002,2020  |
| [4] F.Cichocki et al, Plasma Phys.Control.Fusion <b>66</b> :025015,2024 | [9] W.Eckstein, Vacuum <b>82</b> :930–934,2008   |
| [5] S.Wiesen et al, J.Nucl.Mater. <b>463</b> :480–4,2015                | [10] R.Behrish and W.Eckstein, <i>Sputtering by particle bombardment</i> , Top.Appl.Phys. <b>110</b> ,2010 |